



Effect of methyl substituents on the N-diaryl rings of anthracene-9,10-diamine derivatives for OLEDs applications

Yuan-Hsiang Yu ^{a,*}, Chien-Hsun Huang ^{b,d}, Jui-Ming Yeh ^b, Ping-Tsung Huang ^c

^a Department of Innovations in Digital Living, Lan Yang Institute of Technology, Yilan County 261, Taiwan

^b Department of Chemistry, Center for Nanotechnology at CYCU and R & D Center for Membrane Technology, Chung-Yuan Christian University, Chung Li 32023, Taiwan

^c Department of Chemistry, Fu Jen Catholic University, Hsinchuang, Taipei County 24205, Taiwan

^d Department of Intelligent Materials Technology, Plastics Industry Development Center, Taichung, Taiwan

ARTICLE INFO

Article history:

Received 19 November 2010

Received in revised form 10 January 2011

Accepted 25 January 2011

Available online 23 February 2011

Keywords:

Organic electronics

OLED

Anthracene derivatives

Dopant

ABSTRACT

A series of N-diaryl-anthracene-9,10-diamine derivatives with methyl substituents at *meta* or *para* position of N-diaryl rings were synthesized and used as dopants for Organic Light-Emitting Devices (OLED). The effects of substituted methyl substituents have been compared based on both materials and solid device evaluation. The performance of solid state devices in the configuration of ITO/N,N'-bis(naphthalene-1-yl)-N,N'-bis(phenyl)benzidine (NPB) (40 nm)/3% dopant: 9,10-di(2-naphthyl)anthracene (AND) (40 nm)/tris(8-hydroxyquinoline)aluminum (Alq₃) (20 nm)/LiF (1.5 nm)/Al (200 nm) have been studied. As compared to the non-substituted dopant N,N,N',N'-tetraphenyl-anthracene-9,10-diamine, current efficiency was promoted to approximately 2.9, 6.33, and 7.94 cd/A, and power efficiency was improved by 0.74, 2.26 and 3.02 lm/W, for dopants with the substituted methyl groups at *meta*, *para* and both *meta/para* positions, respectively. The device, prepared by using the dimethyl-substituted dopant at *meta/para* position, showed the best performance when the luminance of the device reached 24,991 cd/m² with CIE (x, y) = (0.38, 0.59), and the efficiency of the device reached 24.99 cd/A and 7.48 lm/W at a driving current of 100 mA/cm². As compared with a device made of a coumarin (C545T)/Alq₃-based emitting layer, the dimethyl-substituted dopant/ADN-based device developed in this study, exhibited great improvement in device performance.

© 2011 Elsevier B.V. All rights reserved.

1. Introduction

Since the first discovery of organic light-emitting devices (OLEDs) by Tang and co-workers [1], materials and devices of OLEDs have drawn much attention due to their potential application in flat panel display [2,3]. Recently, organic light-emitting diodes based on guest/host emitters were found to give extremely excellent high luminance as well as current and power efficiency [4,5]. OLEDs using anthracene derivatives as guest/host emitters have been reported to exhibit very excellent performance and have

potential for fluorescent materials [6–8]. A variety of bulky functional groups have been designed to prevent the intermolecular stacking of anthracene to increase fluorescent quantum yield, device lifetime and color purity [9,10]. In this study, we fabricate the OLEDs based on a guest/host system utilizing different anthracene-9,10-diamine derivatives as dopants, which were incorporated with strategically placed “methyl” steric groups in the structure. The methyl groups were introduced to the aryl ring of N-aryl-substituted anthracene-9,10-diamine derivatives to prevent molecular aggregation of the dopant emitters and reduce self-quenching through steric hindrance of the molecular structure. In addition, the constructed OLEDs were based on a wide band gap host material

* Corresponding author. Tel.: +886 3 9771997x231.

E-mail address: yuyh@mail.fit.edu.tw (Y.-H. Yu).

9,10-di(2-naphthyl)anthracene (AND) [11], which is designed to be used as a host material because it also has the anthracene structure identical to the dopants. Here, both the host and guest contain the anthracene moieties which are supposed to increase the compatibility between guest and host as to have well-dispersed dopants in the host matrix, and lead to an increase in the emission efficiency.

The dopants (with sample code) for OLEDs fabrication were N,N,N',N'-tetraphenyl-anthracene-9,10-diamine (TAD), N,N,N',N'-tetra-*m*-tolyl-anthracene-9,10-diamine (*TmAD*), N,N,N',N'-tetra-*p*-tolyl-anthracene-9,10-diamine (*TpAD*) and N,N,N',N'-tetrakis-(3,4-dimethyl-phenyl)-anthracene-9,10-diamine (*TmpAD*). Among these compounds, the physical properties and device performances of TAD and *TpAD* were already reported as the host emitters [12]. Here, we present the first reported case in which the *N*-diaryl amino anthracenes were used as green dopant in ADN host system for OLED devices. We are reporting on the synthesis, characterization, fabrication and performance of OLED devices that incorporate the four dopant molecules described above in the emitting layer. The effects of substituted methyl group at different positions of aromatic *N*-aryl-substituted anthracene-9,10-diamine have been compared based on both materials and solid device evaluation. Moreover, the device performance of the dimethyl-substituted dopants/AND-based devices was also compared to a general guest/host system based on coumarin (C545T) as dopant and Alq₃ as host [13]. The improvement effect of guest/host both based on anthracene derivatives could be observed in this study.

2. Experimental

2.1. Materials and Instrumentations

Sodium tert-butoxide (*t*-BuONa, Merck), Tri-tert-butylphosphine (P(*t*-Bu)₃, Strem), Palladium(II) acetate (Pd(OAc)₂, Strem), Tris(dibenzylideneacetone)dipalladium (Pd₂(dba)₃, Strem), 9,10-Dibromoanthracene (98%, Alfa), Diphenylamine (98%, Alfa), Di-*m*-tolyl-amine (98%, Alfa), Di-*p*-tolyl-amine (97%, Adrich), 4-Bromo-*o*-xylene (98%, Alfa), Benzylamine (99%, Acros), Palladium (10% on carbon, Alfa), Anthracene (98%, Acros), Ethanol (Merck), *n*-Hexane (Merck), Methanol (Merck) were used as received without further purification. Tetrahydrofuran (THF, Merck), Toluene (SHOWA), Dichloromethane (CH₂Cl₂, Merck) were dried and distilled under standard procedure (THF and Toluene dried using Na/Ph₂CO; CH₂Cl₂ dried using CaH₂) and stored under nitrogen. For device fabrication, 9,10-di(2-naphthyl)anthracene (ADN), copper phthalocyanine (CuPc), N,N'-bis(naphthalene-1-yl)-N,N'-bis(phenyl)benzidine (NPB), 2,3,6,7-tetrahydro-1,1,7,7-tetramethyl-1*H*,5*H*,11*H*-10(2-benzothiazolyl)quinolizine- [9,9a,1g] coumarin (C545T), tris(8-hydroxyquinoline)aluminum (Alq₃) were received from a commercial source (Summit-Tech Co., Ltd.) and purified by a temperature programmed sublimation system. Tungsten boat (Summit-Tech Co., Ltd.), Alumina (Alfa) and LiF (Alfa) were used as received from commercial sources. Indium tin oxide (ITO)-coated

glass substrates with surface resistance 15 Ω/□ were bought from Ritek Co., Ltd.

The synthesized compounds were characterized by Nuclear Magnetic Resonance (NMR) and Mass spectrometer. NMR measurements were made using Bruker AMX 400 and 500 NMR spectrometer. Mass spectra were obtained with a MAT-95XL HRMS mass spectrometer. The UV-visible spectra were recorded using a Perkin Elmer Lambda 35 UV-visible spectrophotometer. Fluorescence spectra were recorded using a Hitachi F-4500 fluorescence spectrophotometer. Photo-electron spectra were obtained by a Riken Keiki Photo-electron Spectrometer model AC-2. Quantum yields were recorded using an integrating sphere and a HAMAMATSU photonic multi-channel analyzer C10027. All data were averaged from at least five raw data to ensure statistical significance. Device properties were monitored using a Keithley 2400 power supply with a 400 nm cut-off filter. An optical meter of model PR705 was used in this study. All of the products were purified by sublimation method with a temperature programmed condition using an upper opened sublimation system made by ULVAC. The high vacuum evaporation system was made by Branchy Technology Co., Ltd. for organic thin film deposition. Thin films were prepared by vacuum evaporation at a base pressure of 2 × 10⁻⁵ Torr or lower. The film thickness was measured with a calibrated quartz-crystal microbalance during deposition.

2.2. General procedure for the synthesis of diaryl-anthracene-9,10-diamine derivatives

The structure of as-synthesized diaryl-anthracene-9,10-diamine derivatives are illustrated in Fig. 1 with compound code TAD, *TmAD*, *TpAD* and *TmpAD*, respectively. The diaryl-anthracene-9,10-diamine derivatives were prepared in high yields, by palladium-catalyzed C–N cross-coupling [12,14–16] of the 9,10-Dibromoanthracene with the amine (Diphenylamine, Di-*m*-tolyl-amine, Di-*p*-tolyl-amine or Bis-(3,4-dimethyl-phenyl)-amine). 9,10-Dibromoanthracene (1 equiv.), Pd(OAc)₂ or Pd₂(dba)₃ (1 mol%), *t*-BuONa (2.5 equiv.), the amine (Diphenylamine, Di-*m*-tolyl-amine, Di-*p*-tolyl-amine or Bis-(3,4-dimethyl-phenyl)-amine) (2.4 equiv.) were weighted into a 500 ml double-neck round-bottom flask connected with a condenser under nitrogen. Dry toluene (200 mL) was then added under nitrogen with stirring to give a homogeneous mixture. A solution containing P(*t*-Bu)₃ (5 mol%) and dry toluene (3.4 mol%) was then added to the mixture and reacted under nitrogen for some hours at 130 °C. The endpoint of reaction was monitored by thin-layer chromatography. After complete consumption of starting materials, the resulting solution was cooled to room temperature; and *n*-hexane was added to precipitate the products. The products were collected by filtering and then dried under vacuum for overnight at 100 °C. The crude products were purified by sublimation method under the programmed condition (e.g. 280 °C for 90 min, 300 °C for 90 min, 320 °C for 90 min and then 100 °C). The detailed synthetic procedures of compounds TAD, *TmAD*, *TpAD* and *TmpAD* were described as follows:

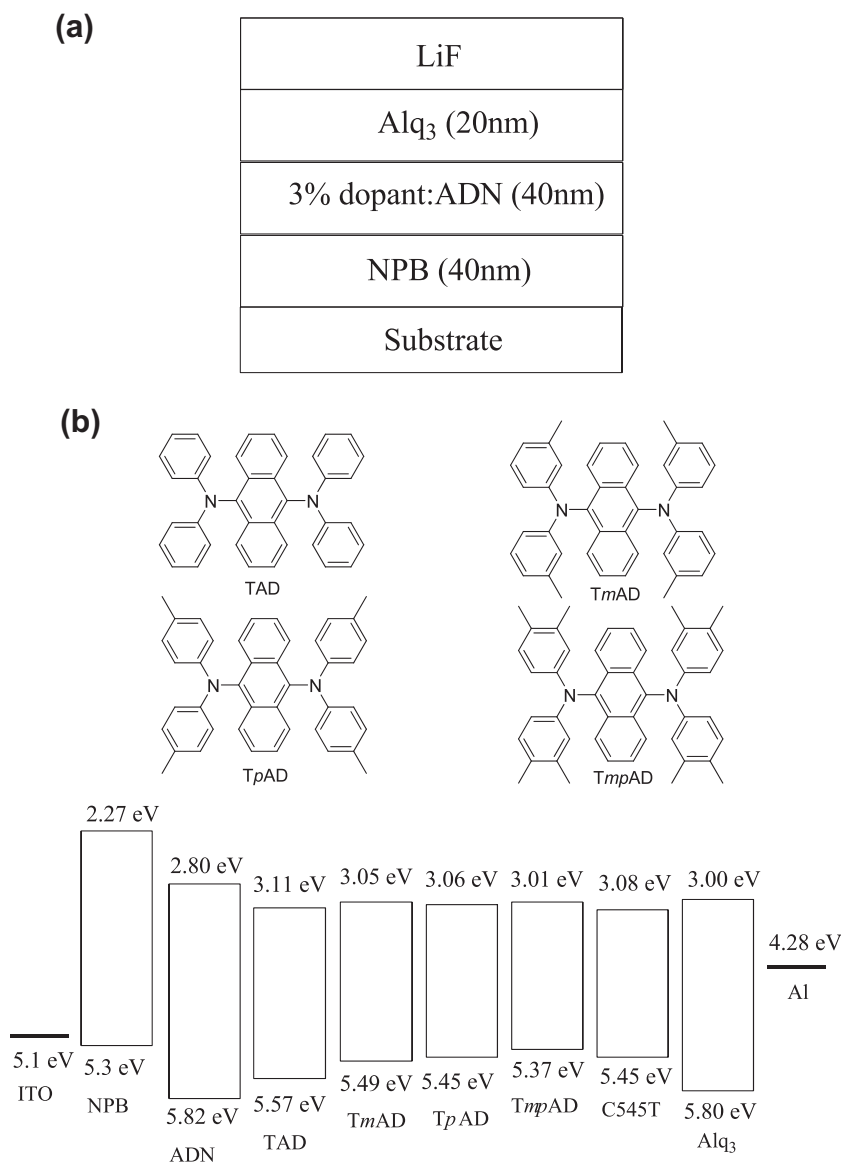


Fig. 1. (a) Schematic OLED device setup. (b) Molecular structure of as-synthesized dopants and relative energy diagram of materials used in all the devices.

2.2.1. *N,N,N',N'*-tetraphenyl-anthracene-9,10-diamine (TAD)

From 9,10-Dibromoanthracene (10 g, 29.8 mmol) and Diphenylamine (12.09 g, 71.4 mmol), compound TAD was obtained as a yellow solid. The crude product was purified twice by sublimation to afford compound TAD in 78% yield. ¹H NMR (400 MHz, CDCl₃): δ = 6.89–6.92 (t, J = 3.2 Hz, J = 7.2 Hz, 4 H), 7.10–7.12 (d, J = 4.4 Hz, 8 H), 7.18–7.22 (t, J = 7.2 Hz, J = 8.4 Hz, 8 H), 7.33–7.36 (q, J = 3.2 Hz, 4 H), 8.17–8.20 (q, J = 3.2 Hz, 4 H); ¹³C NMR (100 MHz, CDCl₃): δ = 120.3, 121.4, 125.1, 126.8, 129.3, 131.8, 137.4, 147.7; EI MS (m/e): 512 (M⁺).

2.2.2. *N,N,N',N'*-tetra-*m*-tolyl-anthracene-9,10-diamine (TmAD)

From 9,10-Dibromoanthracene (5 g, 14.9 mmol) and Di-*m*-tolyl-amine (7.05 g, 35.7 mmol), compound TmAD

was obtained as a yellow solid. The crude product was purified twice by sublimation to afford compound TmAD in 79% yield. ¹H NMR (400 MHz, CDCl₃): δ = 2.19 (s, 12 H), 6.70–6.72 (d, J = 7.2 Hz, 4 H), 6.86–6.88 (d, J = 9.84 Hz, 4 H), 6.94 (s, 4 H), 7.04–7.08 (t, J = 8.0 Hz, J = 7.6 Hz, 4 H), 7.33–7.34 (q, J = 3.2 Hz, 4 H), 8.17–8.17 (q, J = 3.2 Hz, 4 H); ¹³C NMR (100 MHz, CDCl₃): δ = 21.6, 117.7, 120.9, 122.1, 125.1, 126.6, 129.0, 131.9, 137.5, 138.9, 147.9; EI MS (m/e): 568 (M⁺).

2.2.3. *N,N,N',N'*-tetra-*p*-tolyl-anthracene-9,10-diamine (TpAD)

From 9,10-Dibromoanthracene (5 g, 14.9 mmol) and Di-*p*-tolyl-amine (7.05 g, 35.7 mmol), compound TpAD was obtained as a yellow solid. The crude product was purified twice by sublimation to afford compound TpAD

in 82% yield. ^1H NMR (500 MHz, CDCl_3): δ = 2.24 (s, 12 H), 6.98–6.99 (d, J = 1.2 Hz, 16 H), 7.30–7.34 (m, 4H), 8.16–8.19 (m, 4H); ^{13}C NMR (125 MHz, CDCl_3): δ = 20.6, 120.1, 121.1, 126.6, 129.8, 130.3, 131.9, 137.5, 145.6; EI MS (m/e): 568 (M^+).

2.2.4. *N,N,N',N'*-tetrakis-(3,4-dimethyl-phenyl)-anthracene-9,10-diamine (TmPAD)

For the synthesis of TmPAD, the Bis-(3,4-dimethyl-phenyl)-amine was first synthesized as the following procedure: 4-Bromo-*o*-xylene (2 g, 10.8 mmol), Benzylamine (2.54 g, 23.7 mmol), $\text{Pd}_2(\text{dba})_3$ (0.1 g, 1 mol%), *t*-BuONa (2.4 g, 2.3 equiv.) were weighted into a 250 ml double-neck round-bottom flask connected with a condenser under nitrogen. About 50 mL of toluene was added and then stirred to give a homogeneous mixture. A solution of 5 mol% $\text{P}(t\text{-Bu})_3$ in toluene (2.6 mL) was then added to the mixture and reacted at 130 °C. After overnight, the resulting solution was cooled to room temperature, and the solution was evaporated to dryness to afford a powder, which was adsorbed onto 4 g of silica gel and chromatographed with hexane to give 2 g (yield: 80%) of Benzyl-bis-(3,4-dimethyl-phenyl)-amine as a red-brown liquid. The as-prepared Benzyl-bis-(3,4-dimethyl-phenyl)-amine was further reduced to form Bis-(3,4-dimethyl-phenyl)-amine. A mixed solvent of ethanol and THF was added to a 100 mL double-neck round-bottom flask which contained Benzyl-bis-(3,4-dimethyl-phenyl)-amine (2 g, 6.34 mmol) and Pd/C (0.025 g, 2 mol%) and stirred under nitrogen. After the starting materials had dissolved, hydrogen gas was then bubbled into the solution and further reacted overnight. The reaction was monitored by thin-layer chromatography. After the reaction had completed, the resulting brown solution was evaporated to dryness to afford 0.83 g (yield: 58%) of Bis-(3,4-dimethyl-phenyl)-amine as a brown solid which was used as the starting material for the synthesis of compound TmPAD. Compound Benzyl-bis-(3,4-dimethyl-phenyl)-amine was identified by ^1H NMR (400 MHz, CDCl_3): δ = 2.08–2.19 (m, 12 H), 4.30 (s, 2 H), 6.40–6.43 (q, J = 2.4 Hz, 2H), 6.49–6.50 (d, J = 2.0 Hz, 2H), 6.93–6.95 (d, J = 80 Hz, 2H), 7.25–7.38 (m, 5H). Compound bis-(3,4-dimethyl-phenyl)-amine was identified by ^1H NMR (400 MHz, CDCl_3): δ = 2.19–2.20 (d, 12 H), 5.43 (s, 1 H), 6.78–6.82 (m, 4 H), 6.99–7.01 (d, 2H).

From 9,10-Dibromoanthracene (5 g, 14.9 mmol) and Bis-(3,4-dimethyl-phenyl)-amine (8.05 g, 35.7 mmol), compound TmPAD was obtained as an orange solid. The crude product was purified twice by sublimation to afford compound TmPAD in 81% yield. ^1H NMR (400 MHz, CDCl_3): δ = 2.11 (s, 12 H), 2.15 (s, 12H), 6.77–6.80 (q, J = 2.4 Hz, 4 H), 6.91–6.93 (m, 8 H), 7.31–7.33 (q, J = 3.2 Hz, 4 H), 8.17–8.19 (q, J = 3.2 Hz, 4 H); ^{13}C NMR (100 MHz, CDCl_3): δ = 18.9, 20.1, 117.8, 121.4, 125.2, 126.4, 129.0, 130.2, 132.0, 137.2, 137.5, 145.96; EI MS (m/e): 624 (M^+).

2.3. OLED fabrication

Indium tin oxide (ITO)-coated glass substrates were thoroughly cleaned and treated with oxygen plasma. OLEDs were fabricated by using a multiple source thermal evaporation system at a base pressure of 2×10^{-5} Torr or

lower. The deposition rate was 1 Å/s for all organic films. The LiF film, with thickness of 15 Å, was evaporated at a rate of 0.1 Å/s. The Al cathode, with thickness of 200 nm, was deposited at a rate of 5 Å/s.

3. Results and discussion

3.1. Photo-physics studies

The photo-physics properties of as-synthesized methyl groups substituted *N*-aryl anthracene-9,10-diamine derivatives TAD, TmAD, TpAD and TmpAD were studied by UV-visible and fluorescence spectrophotometer. The absorption and emission spectra as illustrated in Fig. 2a and Table 1 show that these compounds in form of solid film have major absorption bands with wavelength maxima (λ_{max}) within 258–268, 296–297, 360–380 and 470–490 nm. The photoluminescence (PL) emission band has λ_{max} located around 519–532 nm. As a result, compound TAD and TmAD have similar emission spectra with $\lambda_{\text{max}} \sim 520$ nm in solid state, whereas there are obvious bathochromic shift observed at $\lambda_{\text{max}} \sim 530$ nm for compound TpAD and TmpAD. The compound TmpAD, with methyl groups substituted in both *para/meta* position, also has similar emission spectra to that of TpAD. The result indicates the methyl group substituted at the *para* position of aromatic phenyl diamine has a greater electronic effect than *meta* position on the anthracene moiety. There is a strong solvent effect for these anthracene materials as illustrated in Fig. 2b and Table 1. Basically the emission color of these compounds exhibit a green color in non-polar solvents, i.e., toluene, and red shift to yellow-green color in polar solvents, i.e., CH_2Cl_2 , for compound with methyl substituents. The solvent effect indicates there is an observable dipole moment between phenyl diamine and anthracene moieties. The dipole moment is strongly dependent on the position of methyl groups at the phenyl diamine, especially for the compound TpAD and TmpAD. The effects of methyl substituents for the comparison of λ_{em} in solvent phase showed the following sequence of TmpAD, TpAD and then TmAD.

A photoelectron spectrometer was used to evaluate the energy of the highest occupied molecular orbital (HOMO). The energy gap (E_g) was calculated by the formula: E_g (eV) = $hc/\lambda_{\text{onset}} = \sim 1241/\lambda_{\text{onset}}$, where h is Planck's constant and c is speed of light. The wavelength onset, λ_{onset} , was obtained by absorption spectra as illustrated in Table 1. The lowest unoccupied molecular orbital (LUMO) was derived from the values of HOMO and E_g , and the data are listed in Table 1. The relative energy diagram of materials used for devices fabrication is compared in Fig. 1 The compound TmpAD has relatively the smallest value of HOMO, i.e. 5.37 eV, due to its higher donor ability than others. The delocalization degree of anthracene relatively decreased along with the donor ability of phenyl diamine moiety, and the energy band gaps become smaller. The energy band gaps follow the sequence: compound TAD > TmAD > TpAD > TmpAD, where the E_g values are 2.46, 2.44, 2.39 and 2.36 eV, respectively.

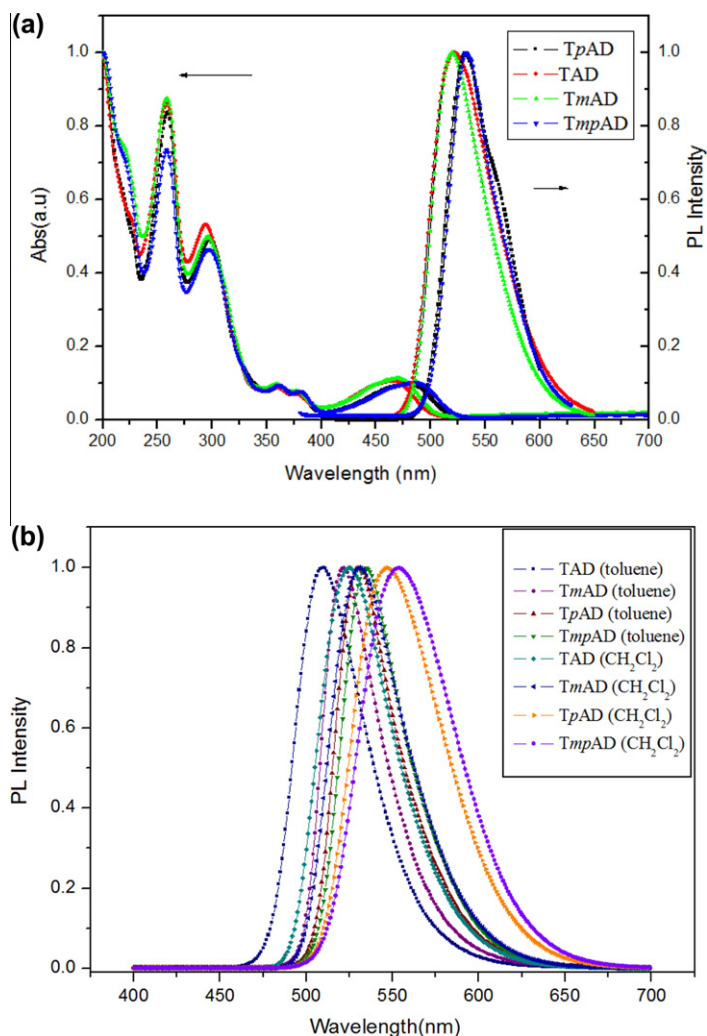


Fig. 2. (a) The absorption and PL spectra of TAD, TmAD, TpAD, and TmpAD in solid film. (b) Solvent effect studies of PL spectra for compound TAD, TmAD, TpAD and TmpAD in toluene and CH₂Cl₂.

Table 1

Relationship of the as-prepared anthracene-9,10-diamine derivatives TAD, TmAD, TpAD, and TmpAD with the λ_{abs} , λ_{onset} , λ_{em} , Q.Y., HOMO, LUMO and Band Gap measured by UV-vis spectrophotometer, fluorescence spectrophotometer, photoelectron spectrometer.

Sample code	λ_{abs} (nm) Film	λ_{onset} (nm) Film	λ_{em} (nm)			Q.Y. ^a	HOMO (eV)	LUMO (eV)	Band Gap (eV)
			Film	Toluene	CH ₂ Cl ₂				
TAD	259, 297, 360, 379, 480	504	520	510	524	0.95	5.57	3.11	2.46
TmAD	258, 296, 360, 379, 469	509	519	521	530	0.92	5.49	3.05	2.44
TpAD	258, 296, 360, 379, 486	519	531	530	546	0.94	5.45	3.06	2.39
TmpAD	268, 296, 360, 379, 486	526	532	535	553	0.82	5.37	3.01	2.36

^a Measured in a CH₂Cl₂ solution by using a HAMAMATSU Photonic multi-channel analyzer C10027.

3.2. Devices fabrication

The as-prepared anthracene-9,10-diamine materials TAD, TmAD, TpAD, and TmpAD were used as dopants of the emitting layer for the application of organic electroluminescent devices. Before device fabrication, compound TpAD was used as a dopant for doping concentration tests

with devices fabricated as follows: ITO/CuPc (15 nm)/NPB (40 nm)/TpAD:AND (40 nm)/Alq₃ (20 nm)/LiF (1.5 nm)/Al (200 nm), where the doping concentration of TpAD was changed between 1 and 4 mol%. It can be seen that the luminance efficiency and brightness of devices were relatively increased by changing the concentration from 1 to 4 mol% as the curves show in Fig. 3. The results show that

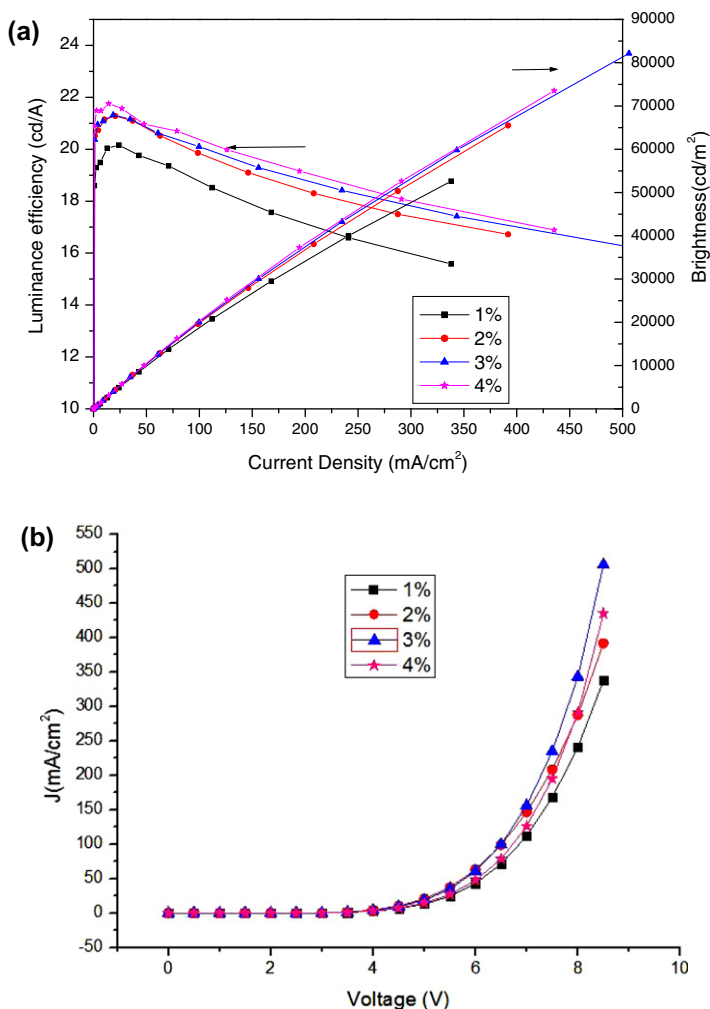


Fig. 3. The doping concentration test with devices fabricated as: ITO/CuPc (15 nm)/NPB (40 nm)/TpAD:AND (40 nm)/Alq₃ (20 nm)/LiF (1.5 nm)/Al (200 nm), where the concentration of TpAD is changed between 1 and 4 mol%.

the devices have good luminance efficiency below a current density of 100 mA/cm^2 . As the current density increased, the optimized concentration of TpAD doping in AND could be compared and selected, where the doping concentration of 3 mol% was the optimum value for considering the driving voltage, luminance efficiency and brightness over a wide range of current density. The result could be observed from the J - V curves for the doping concentration test as shown in Fig. 3b, in which 3 mol% of dopant shows relatively lower driving voltage, when compared at the same current density. Therefore, in this study, a series of solid state devices were fabricated by using 3 mol% dopant for the comparison in the effects of methyl substituents on the dopants.

The structure of devices using the as-prepared anthracene-9,10-diamine derivatives as dopants was designed and fabricated as ITO/NPB (40 nm)/3% dopant:AND (40 nm)/Alq₃ (20 nm)/LiF (1.5 nm)/Al (200 nm) and schematic shown as Fig. 1 Herein, NPB was used as the hole transport layer (HTL). The wide band gap material of AND, which has a high energy band gap of 3.02 eV, was

used as the host material because it might restrict the electron and hole in the emitting layer and was expected to improve the efficiency of emission during recombination. Moreover, the same structure of anthracene moieties for both dopant and the host AND was expected to have more compatible properties and be suitable as a good guest/host combination for the emitting layer. The electron transport layer (ETL) was tris(8-hydroxyquinoline)aluminum (Alq₃).

3.3. Devices properties studies

A comparative device based on a general guest/host system with coumarin (C545T)/Alq₃-based emitting layer was fabricated and named as device 1, which has the structure of ITO/NPB (40 nm)/2% C545T:Alq₃ (40 nm)/Alq₃ (20 nm)/LiF (1.5 nm)/Al (200 nm). The devices based on the as-prepared compound TAD, TmpAD, TmAD, and TpAD were fabricated and named as device 2, device 3, device 4 and device 5, respectively. The device properties are summarized in Table 2. As the results show, device 3 exhibits the best performance with maximal external quantum

efficiency (E.Q.E.) reached to 8.2%. The E.Q.E. values of devices 1–5, which evaluated at 100 mA/cm^2 , follow the sequence: device 3 > device 5 > device 4 > device 2 > device 1, where the E.Q.E. values are 6.91%, 6.37%, 5.40%, 5.33% and 3.52%, respectively. The effects of substituted methyl group at both *para/meta* positions of aromatic *N*-aryl-methyl-substituted 9,10-diaminoanthracene by fabricating the device using the *TmpAD*/AND based guest/host system have been observed with the power efficiency of 9.24 lm/W and current efficiency of 28.17 cd/A , evaluated at luminance of $10,000 \text{ cd/m}^2$. All of the devices have color coordinates located at the green region in the Commission internationale de l'éclairage (CIE) chromaticity diagram. The electroluminescent spectra of devices 1–5 are shown in Fig. 4. Evidently, the trends of emission for these devices are similar to that of solid films as shown in Fig. 2a. For the devices 1–5, the relationships of luminance (B) versus current density (J) are shown in Fig. 5. As shown in B - J curves, the brightness of devices using the dopants with methyl groups at both *para/meta* or *para* positions of *N*-aryl-methyl-substituted 9,10-diaminoanthracene, i.e., the devices 3 and 5, were better than that at *meta* position or non-substituted, i.e., devices 4 and 2. However, all of these developed devices based on the anthracene-9,10-diamine derivatives/AND based guest/host system were greatly enhanced in brightness as compared at the same current density to the system based on coumarin (C545T)/Alq₃ of device 1. Furthermore, as we study the current efficiency (cd/A) or power efficiency (lm/W) related to luminance (cd/m^2), we can find that the curve trends show the device efficiency as follows: device 3 is better than device 5, device 5 is better than devices 4 and 2; device 1 is the worst, as shown in Fig. 6. The improvement in optoelectronic properties of the guest/host system based on anthracene-9,10-diamine derivatives/9,10-di(2-naphthyl)anthracene (AND) as compared to the coumarin (C545T)/Alq₃ is obvious. In addition, the dopant *TmpAD* illustrated the effect of methyl groups substituted at both the *para/meta* posi-

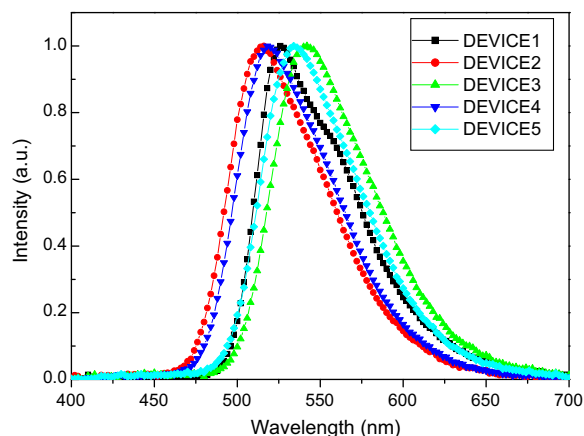


Fig. 4. The electroluminescent spectra of devices fabricated in this study, where device 2–5 with structure of ITO/NPB (40 nm)/dopants: AND (40 nm)/Alq₃ (20 nm)/LiF (1.5 nm)/Al (200 nm), and device 1 (as a compared device) with structure of ITO/NPB (40 nm)/C545T: Alq₃(40 nm)/Alq₃ (20 nm)/LiF (1.5 nm)/Al (200 nm). The dopant of device 2, TAD; device 3, *TmpAD*; device 4, *TmAD*; Device 5, *TpAD*.

tions could greatly improve in device performance. This may be attributed to the relative amorphous property of the emission film and the reduction of the self-quenching phenomena. The steric effect of the two methyl groups substituted at the *meta* and *para* position of phenyl diamine may make the molecules relatively difficult to aggregate with each other. Therefore the emission efficiency can be improved by developing these series of 9,10-diaminoanthracene derivatives as the dopant *TmpAD*. However, the methyl substituents may decrease the carrier mobility and lead to a higher driving voltage as compared with the current density (mA/cm^2) versus driving voltage (V) curves of the fabricated devices as shown as Fig. 7. The driving voltage of device 1 is lower than device 2–5 because of the relatively lower energy barrier between the host

Table 2

The device properties of the as-synthesized anthracene-9,10-diamine derivatives acted as the dopants in the device structure of device 2–5: ITO/NPB (40 nm)/3% dopant:ADN (40 nm)/Alq₃ (20 nm)/LiF (1.5 nm)/Al (200 nm); and compared with the device 1: ITO/NPB (40 nm)/2% C545T:Alq₃ (40 nm)/Alq₃ (20 nm)/LiF (1.5 nm)/Al (200 nm).

	Device 1	Device 2	Device 3	Device 4	Device 5
Dopant	C545T	TAD	<i>TmpAD</i>	<i>TmAD</i>	<i>TpAD</i>
E_L , nm	526	514	542	518	534
CIE (x, y)	(0.34, 0.62)	(0.26, 0.61)	(0.38, 0.59)	(0.29, 0.62)	(0.35, 0.61)
fwhm, nm	66	69	71	68	68
V^a , volt	9.90	10.27	10.49	9.93	10.23
B^a , cd/m^2	13,190	17,048	24,991	19,955	23,378
E_p^a , lm/W	4.19	5.21	7.48	6.31	7.18
E_c^a , cd/A	13.19	17.05	24.99	19.95	23.38
E.Q.E. ^a (%; V)	3.52; 9.90	5.33; 10.27	6.91; 10.49	5.4; 9.93	6.37; 10.23
E.Q.E. ^b (%; V)	4.12; 8.0	6.94; 9.0	8.20; 9.0	5.82; 9.0	6.93; 9.0
I^c , mA/cm^2	74.41	51.81	35.5	49.01	39.63
E_p^c , lm/W	4.45	6.22	9.24	6.96	8.48
E_c^c , cd/A	13.44	19.30	28.17	20.41	25.23

B , luminance; I , current density; V , driving voltage; E_p , power efficiency; E_c , current efficiency; fwhm, full width at half maximum; E.Q.E., external quantum efficiency.

^a evaluated at a current density of 100 mA/cm^2 .

^b the maximum value of E.Q.E.

^c evaluated at luminance of $10,000 \text{ cd/m}^2$.

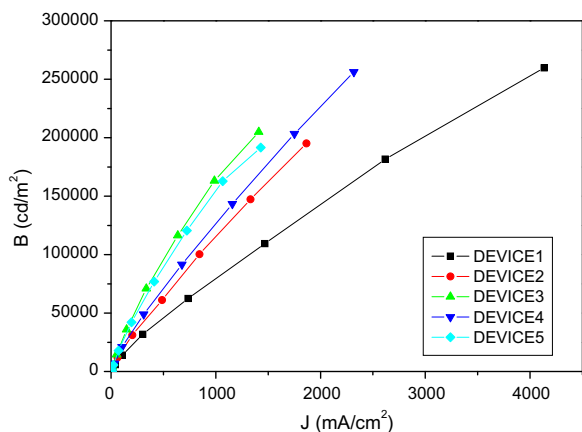


Fig. 5. The relationships of luminance (B) versus current density (J) for the fabricated devices.

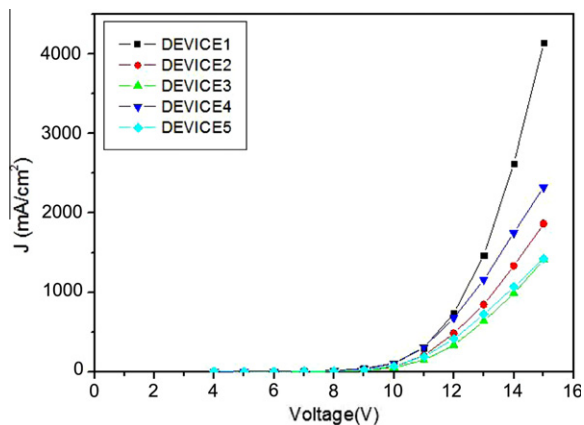


Fig. 7. The current density (mA/cm^2) versus driving voltage (V) measured from the fabricated devices.

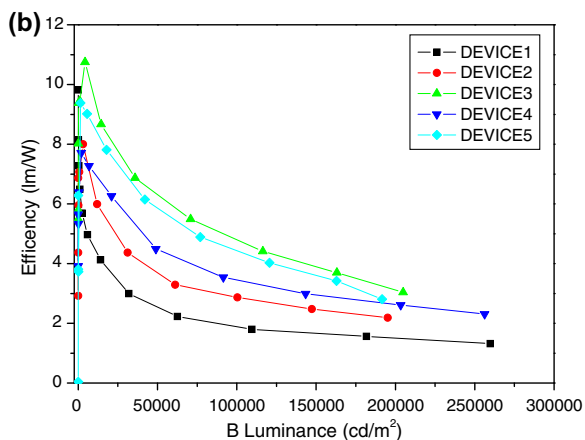
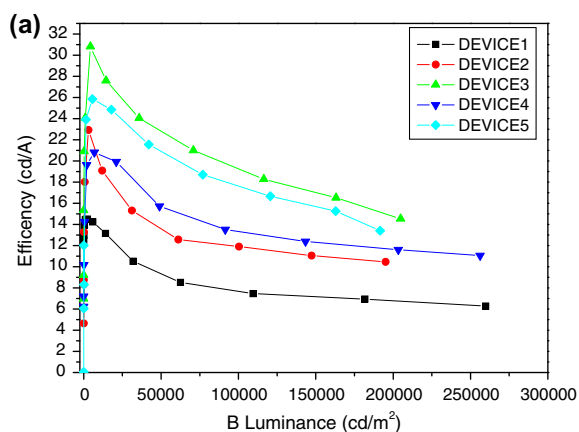


Fig. 6. The relationships of (a) current efficiency (cd/A) and (b) power efficiency (lm/W) relate to luminance (cd/m^2) for the fabricated devices.

emitter layer and the electron transport layer (ETL) as illustrated in Fig. 1. Device 1 has both a host emitter layer and an ETL using material of Alq_3 , while devices 2–5 had been fabricating the host emitter by using AND as to improve the properties of the organic devices. However, a little

higher driving voltage is acceptable as compared to the voltages illustrated in Table 2, e.g., 10.23 volt of device 5 as compared to 9.9 V of device 1.

From the discussion above, we demonstrate the as-prepared compound TAD, *TmAD*, *TpAD*, and *TmpAD*, especially *TmpAD*, could be used as good dopants in the AND based host material for OLEDs fabrication, with excellent electroluminescent properties. In general, their performances are better than coumarins/ Alq_3 based devices, although the driving voltage is a little worse. The methyl substituents on the aromatic ring of phenyl diamine also induce the emission red-shift to closer to the range of eye sensitive wavelength near 550 nm, e.g., 542 nm for *TmpAD*. Therefore, these methyl-substituted dopants are suitable when used as highly efficient green dopant materials for OLEDs.

As compared with device 2 for the effects of methyl substituents in devices efficiency, current efficiency was promoted about 2.9, 6.33, and 7.94 cd/A for dopants with the substituted methyl groups at *meta*, *para* and both *meta/para* position, for device 4, 5 and 3, respectively. In addition, the power efficiency was also significantly increased with 0.74, 2.26 and 3.02 lm/W for device 4, 5, and 3, respectively. When comparing the results, device 3, fabricated by *TmpAD*/AND-based emitter system, exhibits the best E.Q.E., luminance efficiency, power efficiency, and the most saturated green with CIE $x = 0.038$; $y = 0.59$ for OLED applications. We demonstrate that the as-prepared compound TAD, *TmAD*, *TpAD* and *TmpAD*, especially *TmpAD*, could be used as good dopants in the AND based host material for OLEDs fabrication, with excellent electroluminescent properties. In general, their performances are better than coumarins/ Alq_3 based devices.

4. Conclusions

The methyl substituents on the *N*-diaryl rings of anthracene-9,10-diamine showed obvious effects in emission spectra as demonstrated in photo-studies, which observed a significant bathochromic shift followed by the sequence of compound *TmpAD*, *TpAD*, and *TmAD* as compared to TAD. The energy band gaps are relatively decreased as

the methyl groups substituted at the *N*-diaryl rings, especially significant for both on *para/meta* positions of compound *TmpAD*. Here we demonstrate the as-prepared compound TAD, *TmAD*, *TpAD*, and *TmpAD*, especially *TmpAD*, could be used as good dopants in the wide band gap AND based emitting layers for OLEDs fabrication, which have excellent performances better than coumarins/ Alq_3 based devices. The effect of methyl groups substituted at both the *para/meta* positions of the *N*-diaryl rings of anthracene-9,10-diamine could show great improvement in device performance as compared to the non-substituent compound TAD.

Acknowledgements

The financial support of this research by the NSC-96-2622-E-267-001-CC3 is gratefully acknowledged. We thank Professor Ken-Tsung Wong and Miss Shu-Hua Chou at Department of Chemistry of National Taiwan University for the measurement of quantum yields.

References

- [1] C.W. Tang, S.A.V. Slyke, Appl. Phys. Lett. 51 (1987) 913.
- [2] L.S. Liao, K.P. Klubek, C.W. Tang, Appl. Phys. Lett. 84 (2004) 167.
- [3] J. Kalinowski, Organic Light Emitting Diodes: Principles, Characteristics, and Processes, Marcel Dekker, New York, 2005.
- [4] J. Kido, Y. Iizumi, Appl. Phys. Lett. 73 (1998) 2721.
- [5] M.T. Lee, C.K. Yen, W.P. Yang, H.H. Chen, C.H. Liao, C.H. Tsai, C.H. Chen, Org. Lett. 6 (2004) 1241.
- [6] X.-Y. Jiang, Z.-L. Zhang, X.-Y. Zheng, Y.-Z. Wu, S.-H. Xu, Thin Solid Films 401 (2001) 251.
- [7] J.-W. Park, P. Kang, H. Park, H.-Y. Oh, J.-H. Yang, Y.-H. Kim, S.-K. Kwon, Dyes Pigm. 85 (2010) 93.
- [8] K.H. Lee, J.N. You, S. Kang, J.Y. Lee, H.J. Kwon, Y.K. Kim, S.S. Yoon, Thin Solid Films 518 (2010) 6253.
- [9] Y.-J. Pu, A. Kamiya, K.-I. Nakayama, J. Kido, Org. Electron. 11 (2010) 479.
- [10] W.J. Jo, K.-H. Kim, H.C. No, D.-Y. Shin, S.-J. Oh, J.-H. Son, Y.-H. Kim, Y.-K. Cho, Q.-H. Zhao, K.-H. Lee, H.-Y. Oh, S.-K. Kwon, Synth. Met. 159 (2009) 1359.
- [11] H. Tang, X. Wang, Y. Li, W. Wang, R. Sun, Displays 29 (2008) 502.
- [12] M.-X. Yu, J.-P. Duan, C.-H. Lin, C.-H. Cheng, Y.-T. Tao, Chem. Mater. 14 (2002) 3958.
- [13] Khizar-ul Haq, Liu Shan-peng, M.A. Khan, X.Y. Jiang, Z.L. Zhang, Jin Cao, W.Q. Zhu, Curr. Appl. Phys. 9 (2009) 257.
- [14] J.F. Hartwig, Synlett (1997) 329.
- [15] B.H. Yang, S.L.J. Buchwald, Organomet. Chem. 576 (1999) 125.
- [16] A.R. Muci, S.L. Buchwald, Top. Curr. Chem. 219 (2002) 131.